Influenza A surface glycosylation and vaccine design

Chung-Yi Wu[a], Chih-Wei Lin[a], Tsung-I Tsai[a], Chang-Chun David Lee[a], Hong-Yang Chuang[a], Jhih-Bin Chen[a], Ming-Hung Tsai[a], Bo-Rui Chen[a], Pei-Wen Lo[a], Chiu-Ping Liu[a], Vidya S. Shivatare[a], and Chi-Huey Wong[a,1]

[a]Genomics Research Center, Academia Sinica, Taipei 115, Taiwan

Contributed by Chi-Huey Wong, November 16, 2016 (sent for review July 12, 2016; reviewed by Nicola L. B. Pohl and Mark von Itzstein)

We have shown that glycosylation of influenza A virus (IAV) hemagglutinin (HA), especially at position N-27, is crucial for HA folding and virus survival. However, it is not known whether the glycosylation of HA and the other two major IAV surface glycoproteins, neuraminidase (NA) and M2 ion channel, is essential for the replication of IAV. Here, we show that glycosylation of HA at N-142 modulates virus infectivity and host immune response. Glycosylation of NA in the stalk region affects its structure, activity, and specificity, thereby modulating virus release and virulence, and glycosylation at the catalytic domain affects its thermostability; however, glycosylation of M2 had no effect on its function. In addition, using IAV without the stalk and catalytic domains of NA as a live attenuated vaccine was shown to confer a strong IAV-specific CD8$^+$ T-cell response and a strong cross-strain as well as cross-subtype protection against various virus strains.

influenza A virus | glycosylation | vaccine design

Influenza A viruses (IAV) belong to the Orthomyxoviridae family and can circulate widely and cross interspecies barriers through the highly antigenic drift and shift of the 18 subtypes of HA and 11 subtypes of neuraminidase (NA) (1, 2). In addition, the posttranslational modification of the IAV surface proteins is important to circumvent host defense and support the virus life cycle (3).

HA is a major surface glycoprotein of IAV and is involved in viral infection via binding to sialic acid (SA)-containing glycans on the surface of host cell (3). The other major glycoprotein of IAV, NA, is involved in the cleavage of SA on the host cell receptor to facilitate the release of viral particles to infect other cells (4). M2, the third surface protein of IAV, has ion channel activity to regulate virus penetration and uncoating (1). All surface proteins interact with M1 protein for virus assembly and release (5).

The modification of HA and NA by N-glycosylation is important in the IAV life cycle (1, 6–8). Previously, we have shown that the glycosylation of HA affects its receptor binding, immune response, and structural stability, and glycosite 27 is essential for retaining the structural integrity of HA and its receptor binding (6, 9). In addition, using the monoglycosylated HA as immunogen, it showed a broader protection against various IAV subtypes compared with the fully glycosylated version (10). However, it is not clear whether the other specific glycosites and their glycan structures on HA regulate its functions. With regard to NA, the functional roles of its glycosylation are not well understood, though N-glycosylation was reported to stabilize the protein from protease digestion and may affect the enzyme activity (11, 12). The aim of this study was to understand the functional effects of glycosylation on HA, NA, and M2, and how glycosylation of the surface proteins affects the life cycle of IAV.

Results

Glycosylation of HA at N-142. Because several glycosylation sites (glycosites 27, 40, 176, 303, and 497) on HA are highly conserved among the H1, H3, and H5 subtypes (9), we used wild-type H1N1 A/WSN/33 (WSN) as a model to create or delete specific glycosites to address the effect of glycosylation by using reverse genetics (Fig. 1*A* and Fig. S1*A*). We found that the virus could not survive with glycosite-27 deletion (i.e., N27A mutation designated as 27-G), consistent with our previous finding that glycosylation at glycosite 27 played a key role in HA folding (6). Similarly, we also mutated the highly conserved and potential glycosite at position 40, 176, or 303 to Asn (designated as 40 + G, 176 + G, and 303 + G) and evaluated the effect on replication. The results showed that the replication rates of variants with mutation at the highly conserved or potential glycosite (40 + G, 176 + G, 303 + G, or 497 − G) and WT were similar, but the replication rate of glycosite 142-deleted virus (142-G and 142-285-497-556-G virus) was two orders of magnitude lower than that of the WT virus in both Madin-Darby canine kidney cells (MDCK) and A549 cells, suggesting that glycosite 142 plays an important role in IAV replication (Fig. 1*B* and Fig. S1*B*). In a circular dichroism study, the glycans at glycosite 142 did not affect the secondary structure of HA (Fig. S1*C*), and the ratios of HA to M1 among the glycosite 142-deleted variants were similar, suggesting that glycosite 142 is not essential for virus assembly and/or maturation (5) (Fig. S1*D*).

In the course of understanding the effect of glycosite 142 deletion on the life cycle of IAV, we found that glycosite 142 is very important for virus entry, because in the virus infectivity assay, very weak signals of HA and M1 were detected in the A549 cells infected with glycosite 142-deleted virus (142-G or 142-285-497-556-G virus; Fig. 1*C* and Fig. S1*E*). The glycan array analysis showed that the glycosite 142-deleted virus interacted with more sialosides than the WT virus (glycans 8, 10, 11, and 15–18), and the same results were also observed from the corresponding HA protein, suggesting that glycosylation at glycosite 142 affects the receptor binding specificity of HA (Fig. 1*D* and Fig. S2 *A*–*C*). In addition, glycosite 142 modulates the binding avidity of HA, because the glycosite 142-deleted virus showed lower fluorescence intensity in glycan array analysis, and had lower capability in hemagglutination and cell binding (Fig. 1 *D* and *E* and

Significance

Influenza A virus (IAV) is a major threat to global public health, and so understanding the biology of IAV is essential to develop antiflu vaccines and therapeutics. Here, we show the links between viral surface glycosylation and IAV function. The glycosylation of HA modulates virus infectivity, and host immune response; the glycosylation of NA affects its structure, activity, specificity, and thermostability to regulate virus release and virulence. In addition, using live attenuated IAV without the stalk and catalytic domains of NA as vaccine can strongly induce IAV-specific CD8$^+$ T-cell responses to various virus strains. Therefore, our findings have clarified the role of glycosylation in IAV and provided a new direction for the development of universal flu vaccines.

Author contributions: C.-Y.W. and C.-H.W. designed research; C.-Y.W., C.-W.L., T.-I.T., C.-C.D.L., H.-Y.C., J.-B.C., M.-H.T., B.-R.C., P.-W.L., and C.-P.L. performed research; C.-Y.W. and C.-H.W. analyzed data; and C.-Y.W., V.S.S., and C.-H.W. wrote the paper.

Reviewers: N.L.B.P., Indiana University; and M.v.I., Griffith University.

Conflict of interest statement: A provisional patent application on this work has been filed.

[1]To whom correspondence should be addressed. Email: chwong@gate.sinica.edu.tw.

This article contains supporting information online at www.pnas.org/lookup/suppl/doi:10.1073/pnas.1617174114/-/DCSupplemental.

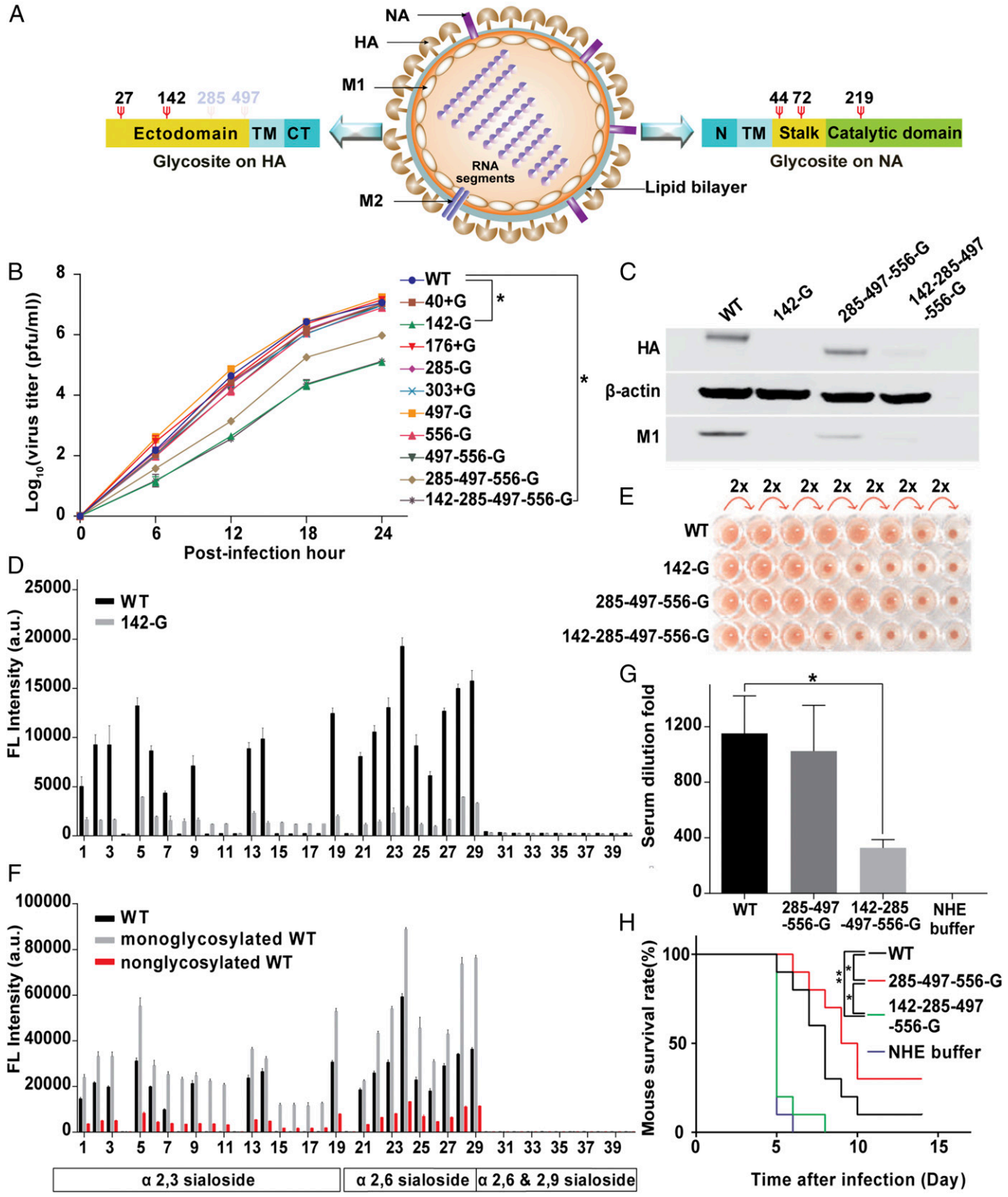

Fig. 1. HA glycosylation and IAV. (*A*) Schematic overview of glycosites (red Ψ) on IAV surface proteins. CT, C-terminal cytoplasmic domain; N, N-terminal cytoplasmic domain; TM, transmembrane domain. (*B*) Comparison of virus replication rates in MDCK cells. (*C*) Western blot analysis of A549 cells infected with four variants of IAV and the total lysates were collected to run SDS/PAGE at 10 hpi. The filter was probed with anti-HA, anti-M1, and anti–β-actin antibodies. (*D*) HA binding patterns in a glycan array from WT and 142-G. (*E*) Hemagglutination assay of IAV variants. (*F*) Glycan array analysis of deglycosylated HA WT viruses. (*G*) Mice were immunized with inactivated viruses as indicated in the figure, and the sera of immunized mice were then analyzed using hemagglutination inhibition assay. (*H*) The mouse survival rate was measured after challenge with a lethal dose of H5N1 viruses. (*B*, *D*, and *F*) Mean ± SEM for three independent experiments. (*G* and *H*) Mean ± SEM for 10 independent experiments. $^{*}P < 0.001$. $^{**}P < 0.05$.

Fig. S1*F*). Although the glycosite 142-deleted virus can interact with more α2,3-sialosides in the glycan array analysis, it is not involved in the human and/or avian adoption of WSN HA, because the replication rate of 142-G or 142-285-497-556-G virus in LMH cell lines (from chicken hepatocellular carcinoma) was still two orders of magnitude lower than that of WT (Fig. S1*G*).

The molecular mechanism of avidity and specificity affected by the glycosylation at glycosite 142 was further studied and it was found that both avidity and specificity were modulated by the glycan composition. Treatment with a mixture of endoglycosidases (Endo-F1, F2, F3, and H) changed the interaction profile of the WT and 285-497-556-G viruses on the glycan array and the interaction patterns were similar to that of the 142-G and the 142-285-497-556-G viruses. Surprisingly, after treatment with the endoglcosidase mixture, the fluorescence intensity of the monoglycosylated virus on the glycan array was increased, but decreased in all types of nonglycosylated variants (PNGase F treatment; Fig. 1*F* and Figs. S1*H* and S2 *D* and *E*).

To study whether glycosite 142 is involved in the host immune response, we challenged mice with H5N1. The mice immunized with the inactivated 142-285-497-556-G virus survived for a shorter period and induced less HA antiserum compared with the mice immunized with inactivated WT virus, and the inactivated 285-497-556-G virus-immunized mice induced the same amount of HA antiserum but survived longer, and survived well in all cases after WSN challenge in the immunogenicity test (Fig. 1 *G* and *H* and Fig. S1*I*). This study suggests that glycosylation at glycosite 142 is important for the immunogenicity of IAV.

Glycosylation of NA and M2. To understand whether NA glycosylation is involved in the life cycle of IAV, the same virus strain A/WSN/33 was used as a model for investigation of each glycosite by using reverse genetics (Fig. S3*A*). It was found that glycosites 44 and 72 (in the stalk domain) played an important role in virus replication, and the replication rate of the virus with deleted glycosites 44 and 72 (44-72-G or 44-72-219-G virus) was two orders of magnitude lower than the WT virus in both MDCK and A549 cells (Fig. 2*A* and Fig. S3*B*). Glycosites 44, 72, and 219 on NA were glycosylated to form variants of NA proteins with different molecular weights, but these variants showed similar molecular weights after treatment with the endoglycosidase mixture in Western blot analysis and gel filtration. (Fig. 2B and Fig. S3 *C* and *D*). Interestingly, the secondary structures of these variants were slightly different, but became the same after deglycosylation (Fig. 2 *C* and *D*). These results suggest that the glycans attached to glycosites 44, 72, and 219 are heterogeneous and affect the secondary structures of NA.

Glycans at N-44 and N-72 Affect NA Activity and Virulence. The glycans at glycosites 44 and 72 were also found to be important for the NA activity. The viruses without glycosites 44 and 72 (44-72-G and 44-72-219-G) showed significantly lower NA activity than the WT based on an assay using 2-(4-methylumbelliferyl)-α-D-*N*-acetylneuraminic acid (4-MUNANA) as substrate (Fig. 2*E*). In addition, after the WT virus was treated with the endoglycosidase mixture, the molecular weight and NA activity were lower than that of the untreated virus (Fig. S3 *E* and *F*).

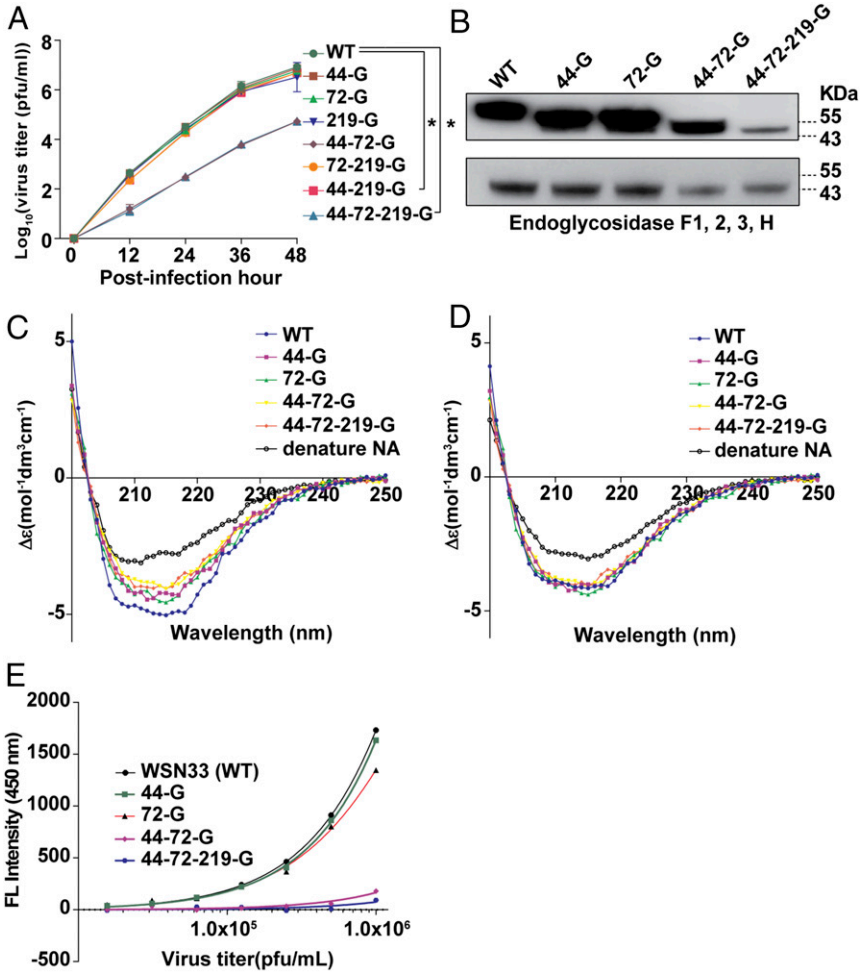

Fig. 2. NA glycosylation and IAV. (*A*) Comparison of virus replication rates in A549 cells. (*B*) Western blot analysis of the molecular weights of glycosylated and deglycosylated variants as indicated. The filter was probed with anti-NA antibody. Mean ± SEM for three independent experiments. (*C*) Circular dichroism spectra of different types of NA as indicated. (*D*) Circular dichroism spectra of deglycosylated variants of NA. (*E*) NA activity of IAV measured by 4-MUNANA assay. Mean ± SEM for five independent experiments. *$P < 0.001$.

The glycans on NA affected the enzyme activity, affinity, and specificity, as the V_{max} and the affinity value (K_m) for different substrates were altered. When 2′(4-meyhylumbelliferyl)-α-D-*N*-acetylneuraminic acid (4-Muα-Neu5Ac), and 6′-sialyl-*N*-acetyllactosamine (6-SLN) were used as substrates, the NA without glycosites 44 and 72 had lower neurominidase activity but the K_m values of all mutants were similar. Surprisingly, when 3-SLN was used as substrate, the activity of NA with glycosite 44 or 72 deleted decreased about 50%, but the K_m value increased more than twofold (Fig. 3*A* and Table S1). Interestingly, the virus production rates of these variants in LMH cells were related to the NA activity on 3-SLN, which is an avian receptor (13) (Fig. 3*B*), suggesting that glycosylation on NA affected IAV replication in mammal and avian cells differently (Figs. 2*A* and 3*B*). In addition, whereas the NA without glycosite 72 (72-G) could interact with 6′-sialyllactose (6-SL) as substrate, none of the variants could interact with 3′-sialyllactose (3-SL; Fig. 3*C* and Fig. S4*A*). Interestingly, the activity of 44-72-219-G was similar to that of 44-72-G (with glycosite 219) from 25 to 40 °C, but lower at higher temperatures (45, 50, and 55 °C; Fig. S4*B*). After 44-72-G was treated with the endoglycosidase mixture, the activity of NA was lower than that without treatment at 55 °C, suggesting that the glycans on glycosite 219 (in the catalytic domain) affect the thermostability of NA (Fig. 3*D* and Fig. S4*C*).

Glycosites 44 and 72 also modulate the virus release and morphogenesis, because the cells infected with WT, 44-G, and 72-G viruses released many more spherical viral particles, but the cells infected with the 44-72-G or the 44-72-219-G virus produced mainly elongated and filamentous shaped particles, which were not observed in the WT virus-infected cells (Fig. 3 *E* and *F* and Fig. S4 *D*–*F*). In addition, mice infected with viruses without any glycans on NA (44-72-219-G virus) showed less-prominent changes in survival rate and body weight compared with the WT-infected mice, which had a 20% survival rate and considerable loss of body weight, suggesting that the glycosylation on NA affected virulence (Fig. 3 *G* and *H*).

Live Attenuated Vaccine Without the Stalk and Catalytic Domains of NA Showed Broad Protection With Strong CD8$^+$ T-Cell Response. To study whether the NA activity would affect host immune response and its potential as live attenuated influenza vaccine (LAIV), we used the virus with nonglycosylated NA (44-72-219-G virus) as

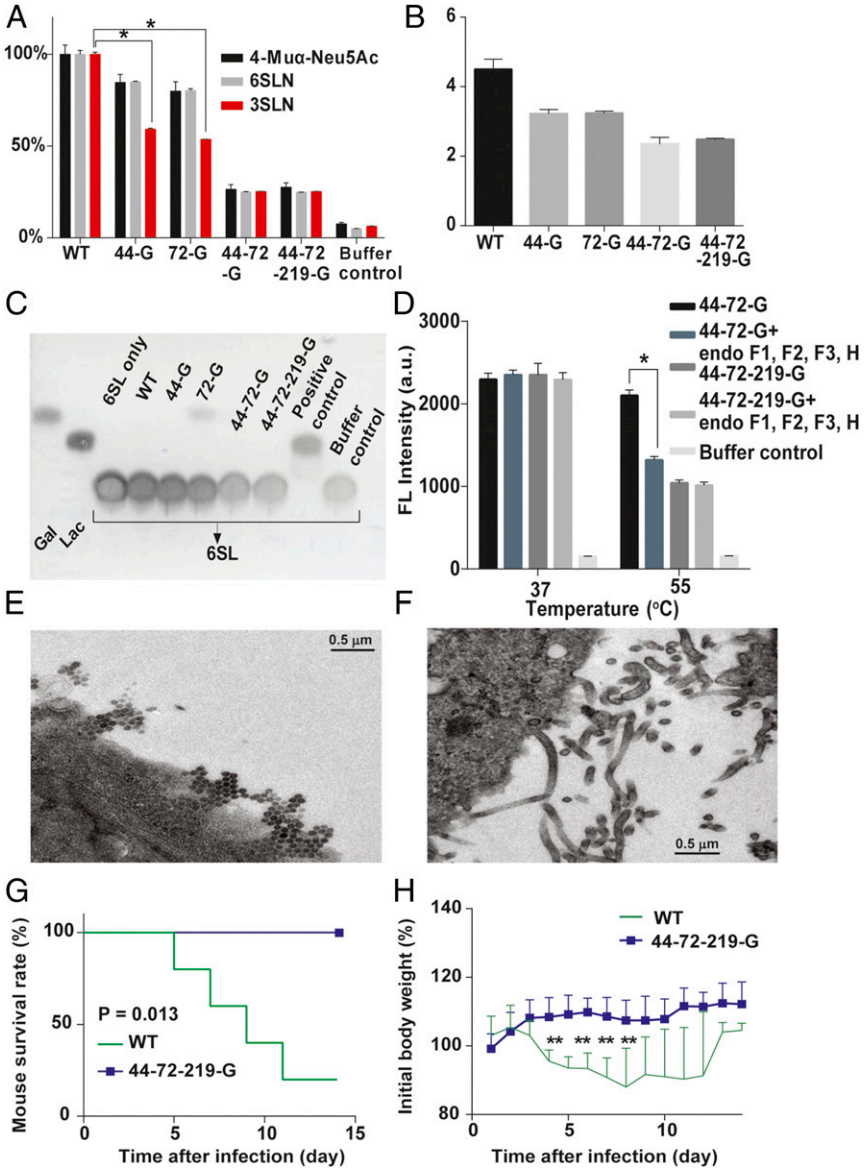

Fig. 3. Characterization of viruses with different glycosylation patterns on NA. (*A*) Measurements of NA activity using different glycoconjugates, 4-Muα-Neu5Ac, 6-SLN, and 3-SLN; the NA activity was relative to each WT substrate designated as 100%. (*B*) Comparison of virus production in chicken hepatocellular carcinoma cells (LMH cells). The virus titers were determined at 48 hpi. (*C*) TLC of variants of viruses that interact with 6-SL. (*D*) The 4-MUNANA assay was used to measure the NA activity of 44-72-G virus, deglycosylated 44-72-G virus, and 44-72-219-G virus at 37 and 55 °C. (*E*) Viral morphology as examined by transmission electron microscopy for WT virus. (*F*) 44-72-219-G virus. (*G*) After mice were infected with WT and glycosylation-defective NA virus (44-72-219-G), survival rate and (*H*) body weight were recorded for 14 d. (*A*, *B*, and *D*) Mean ± SEM for three independent experiments. (*G* and *H*) Mean ± SEM for five independent experiments. *$P < 0.001$. **$P < 0.05$.

LAIV (LAIV WSN-44-72-219-G) because it had low NA activity and virulence. However, the nonglycosylated NA virus showed a similar immunogenicity as WT (Fig. S5). In addition, the NA activity had no effect on the efficiency of inactive vaccine, and the level of antibody produced was very low (14, 15). Therefore, in an attempt to enhance the immunogenicity of NA, we generated a virus without both the stalk and catalytic domains of NA (LAIV WSN-NA) by adding a stop codon to the RNA genome segment of NA (Fig. 4*A*). It was found that LAIV WSN-NA virus did not form the plaque in MDCK cells and could be rescued by expressing WT NA in the cell (Fig. S6 *A* and *B*). After 24 hours after postinfection (hpi), the A549 cells infected by LAIV WSN-NA virus showed fewer viruses released into the supernatant, and the intracellular viral protein M1 was accumulated, suggesting that LAIV WSN-NA virus had a defect in virus release (Fig. S6 *C* and *D*). The body weight of mice infected with 1×10^6 pfu of WSN viruses rapidly decreased, and these mice died at 6 d postinfection. However, the mice infected with 1×10^6 pfu of LAIV WSN-NA viruses via oral administration survived well and showed no body weight loss, indicating that LAIV WSN-NA virus is an effective LAIV with low pathogenicity, and attenuation of viruses in cells is essential for the efficacy of live vaccine (Fig. S6 *E* and *F*) (16). The immunogenicity of inactivated WSN-NA virus was similar to that of inactivated WSN virus in the immunogenicity test (Fig. 4*B* and Fig. S7). However, when LAIV WSN-NA virus was used as vaccine, it showed cross-strain and cross-subtype protection against WSN, A/Cal/07/2009, and H5N1 in the virus challenge study; the LAIV WSN-NA–treated mice survived well and cleared viruses from the lung, but did not induce any notable antibody response (Fig. 4 *C–E* and Fig. S8 *A–D*). In addition, the protective ability of LAIV WSN-NA also showed a dose-dependent response (Fig. S8*E*). After the virus infected the peripheral blood mononuclear cells (PBMC) from LAIV WSN-NA–treated mice, $CD8^+$ T cells were specifically activated via IFN-γ and granzyme B expression, but the inactive virus did not show this activity, suggesting that LAIV WSN-NA can induce $CD8^+$ T-cell activation upon virus infection (Fig. 4*E* and Fig. S8 *F* and *G*). Furthermore, the highly conserved viral epitopes NP and M1 could also stimulate $CD8^+$ T-cell activation (17) (Fig. 4*G* and Fig. S8*G*). These results suggest that NA plays a key role in regulating the host immune response via $CD8^+$ T-cell activation and LAIV WSN-NA is an effective vaccine.

Finally, we found that there was one glycosite on M2, but it did not affect virus replication (Fig. S9).

Discussion

In the seasonal H1N1 strains, glycosite 142 is believed to play a significant role in evading the human immune response (8), and human H3N2 IAV also gains the glycosite in this region (glycosite 144 in H3 numbering) during evolution through positive selection (18). Surprisingly, we found that after IAV acquired glycosite 142, the efficiency of virus infectivity was promoted by the regulation of the HA–SA interaction, and the host immune response was altered. Therefore, we believe that glycosite 142 is an important factor that should be considered in the development of vaccines against human IAV.

Several studies have suggested that diversification in the stalk domain of NA is associated with the virulence and transmission of IAV, from ducks to land-based poultry, and its spread among humans via evolutionary processes, including sequence deletion and glycosite modification. However, the structural and functional roles of the stalk domain of NA were unknown thus far, and there was no report about the glycosylation of these canonical glycosites (19–23). In this study, we prove that the glycosites in the stalk domain of NA are glycosylated to regulate the activity, affinity, and specificity of NA to modulate IAV replication, suggesting that the glycans in the stalk domain of NA play an important role in the virulence and transmission of IAV.

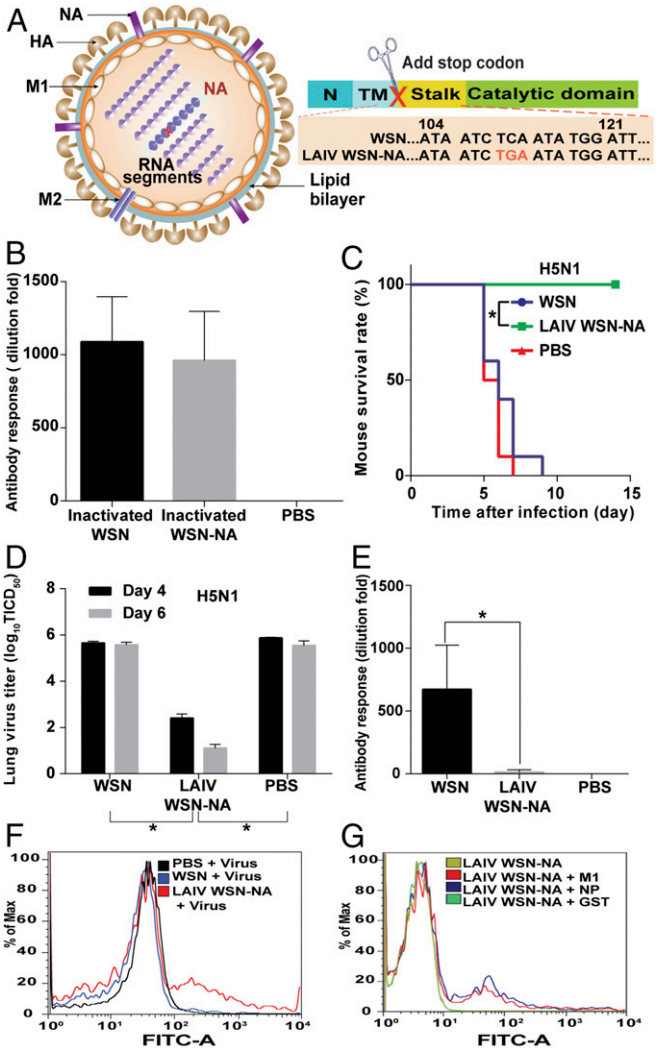

Fig. 4. Immunogenicity of LIAV WSN-NA. (*A*) Schematic overview of the LAIV WSN-NA design. The stalk and catalytic domains of NA were deleted by adding a stop code to the stalk domain of the RNA genome segment of NA, so the cells infected by the WSN without the stalk and catalytic domain cannot translate the stalk and catalytic domains of NA. Numbers refer to the nucleotide numbers from the 5′ end of the cRNA. Red TGA was the stop codon. N, N-terminal cytoplasmic domain; TM, transmembrane domain. (*B*) The sera of mice immunized with inactivated viruses as indicated were analyzed by using hemagglutination inhibition assay. (*C*) Analysis of the survival rate of WSN, LAIV WSN-NA, or PBS treatment mice after challenge with a lethal dose of H5N1. (*D*) H5N1 virus replication kinetics in the lungs of the treated mice as indicated on 4 and 6 postinfection days. (*E*) The sera of the treated mice were analyzed using hemagglutination inhibition assay to measure the antibody level. (*F*) After PBMC from WSN-, LAIV WSN-NA-, and PBS-treated mice were incubated with WSN virus (+virus), the analysis of INF-γ expression in $CD8^+$ T cells was measured by flow cytometry. (*F*) Representative flow cytometry histograms of INF-γ expression in $CD8^+$ T cells from LAIV WSN-NA–treated mice stimulated by M1 and NP epitopes. (*B*, *D*, and *E*) Mean ± SEM of 10 independent experiments. (*C*) Ten independent experiments are shown. (*F* and *G*) Data are representative of three similar experiments. $*P < 0.001$.

However, the relationship between NA activity and the diversity of the stalk domain, and whether the virus release is regulated by the glycosylation in the stalk domain is still unknown (24, 25). Our study here revealed that NA glycosylation is important for IAV virulence and transmission.

Recent development of universal influenza vaccines is focused on the use of conserved peptides or proteins as antigens with

different adjuvants and administration methods to induce immune response (26–29). Expression of the conserved regions of IAV proteins by using viral vector systems can induce $CD8^+$ T cells against lethal IAV challenge in animals, but it still only recognizes one target (30). Another type of vaccine based on the mixture of MVA-NP and M1 was also reported (31). In this study, the IAV without the stalk and catalytic domains of NA was found to significantly induce IAV-specific $CD8^+$ T cells that recognize various strains and different subtypes of IAV in the absence of neutralizing antibodies. Although it is known that human IAV-specific $CD8^+$ T cells provide cross-protection against influenza (32), it is important to further understand how the stalk and catalytic domains of NA affect host immune response. We believe that our findings provide an understanding of glycosylation on influenza cell surface and an innovative direction for the design of a universal influenza vaccine (33, 34).

Materials and Methods

Generation of Recombinant Viruses. Eight fragments of A/WSN/33 viral genome were amplified by RT-PCR. We used the putative sequon N-X-S/T to create (from different amino acid to N) or delete (from N to A) the glycosites in the HA genome, and added a stop codon in the NA genome to remove the stalk and catalytic domain of NA by using site-directed mutagenesis. The viral cDNAs were inserted into pcDNA3.1 containing the pol I and CMV promoter similar to the generation of pHW2000. Recombinant viruses were generated by the eight-plasmid cotransfection method into MDCK/293T cells according to the published protocol (35). Supernatants were collected, titrated, and frozen at −80 °C until use. For the preparation of virus without NA stalk and catalytic domains (LAIV WSN-NA), we generated NA expression-stable MDCK/293T cell lines to rescue, maintain, and analyze the virus (16). Briefly, full-length NA (from WSN strain) was cloned to a cDNA expression lentivector (pLAS2w.Ppuro) to generate NA-expression lentivirus using the protocol provided by the National RNAi Core Facility, Academia Sinica, Taiwan (rnai.genmed.sinica.edu.tw). HEK293T and MDCK cells were infected with NA-expression lentivirus with triple multiplicity of infection in the presence of Polybrene (Sigma) at a final concentration of 8 μg/mL. Cells were incubated with virus for 24 h before replacing the medium with selective medium containing puromycin (3 μg/mL; Invitrogen). After a 3-d incubation, total cell lysate was collected to check the expression efficiency of NA by Western blot analysis.

Mice Treated with LAIV WSN-44-72-219-G and LAIV WSN-NA. LAIV WSN-NA virus was cultured in MDCK cells with NA expression. A total of 25 μL of LAIV WSN-44-72-219-G or LAIV WSN-NA (nonlethal dose for WT WSN) were introduced into each nostril on days 0 and 21 while the mouse was conscious and the virus did not reach the lower respiratory tract. Then the immunogenicity test procedure was performed as described in *SI Materials and Methods* (14).

All animal experiments were evaluated and approved by the Institutional Animal Care and Use Committee of Academia Sinica. More details are provided in *SI Materials and Methods*.

ACKNOWLEDGMENTS. We thank Dr. Jia-Tsrong Jan's laboratory for mouse vaccination and challenge experiments, and Dr. Michael M. C. Lai for providing plasmids for the reverse genetics study. The pLAS2w.Ppuro vector was obtained from the National RNAi Core Facility at Academia Sinica. The Transmission Electron Microscope was from the imaging core in the Institute of Molecular Biology, Academia Sinica. Financial support was provided by Academia Sinica.

1. Medina RA, García-Sastre A (2011) Influenza A viruses: New research developments. *Nat Rev Microbiol* 9(8):590–603.
2. Tong S, et al. (2013) New world bats harbor diverse influenza A viruses. *PLoS Pathog* 9(10):e1003657.
3. Air GM (2014) Influenza virus-glycan interactions. *Curr Opin Virol* 7:128–133.
4. Doyle TM, et al. (2013) The universal epitope of influenza A viral neuraminidase fundamentally contributes to enzyme activity and viral replication. *J Biol Chem* 288(25):18283–18289.
5. Wu CY, Jeng KS, Lai MM (2011) The SUMOylation of matrix protein M1 modulates the assembly and morphogenesis of influenza A virus. *J Virol* 85(13):6618–6628.
6. Liao HY, et al. (2010) Differential receptor binding affinities of influenza hemagglutinins on glycan arrays. *J Am Chem Soc* 132(42):14849–14856.
7. Wagner R, Wolff T, Herwig A, Pleschka S, Klenk HD (2000) Interdependence of hemagglutinin glycosylation and neuraminidase as regulators of influenza virus growth: A study by reverse genetics. *J Virol* 74(14):6316–6323.
8. Wei CJ, et al. (2010) Cross-neutralization of 1918 and 2009 influenza viruses: Role of glycans in viral evolution and vaccine design. *Sci Transl Med* 2(24):24ra21.
9. Wang CC, et al. (2009) Glycans on influenza hemagglutinin affect receptor binding and immune response. *Proc Natl Acad Sci USA* 106(43):18137–18142.
10. Chen JR, et al. (2014) Vaccination of monoglycosylated hemagglutinin induces cross-strain protection against influenza virus infections. *Proc Natl Acad Sci USA* 111(7):2476–2481.
11. Liu P, Wang Z, Zhang L, Li D, Lin J (2015) The mechanism by which 146-N-glycan affects the active site of neuraminidase. *PLoS One* 10(8):e0135487.
12. Tumpey TM, et al. (2005) Characterization of the reconstructed 1918 Spanish influenza pandemic virus. *Science* 310(5745):77–80.
13. Yang H, Carney PJ, Chang JC, Villanueva JM, Stevens J (2015) Structure and receptor binding preferences of recombinant hemagglutinins from avian and human H6 and H10 influenza A virus subtypes. *J Virol* 89(8):4612–4623.
14. Miller MA, Ganesan AP, Luckashenak N, Mendonca M, Eisenlohr LC (2015) Endogenous antigen processing drives the primary CD4+ T cell response to influenza. *Nat Med* 21(10):1216–1222.
15. Monto AS, et al. (2015) Antibody to influenza virus neuraminidase: An independent correlate of protection. *J Infect Dis* 212(8):1191–1199.
16. Watanabe S, Watanabe T, Kawaoka Y (2009) Influenza A virus lacking M2 protein as a live attenuated vaccine. *J Virol* 83(11):5947–5950.
17. Boon AC, et al. (2002) The magnitude and specificity of influenza A virus-specific cytotoxic T-lymphocyte responses in humans is related to HLA-A and -B phenotype. *J Virol* 76(2):582–590.
18. Suzuki Y (2011) Positive selection for gains of N-linked glycosylation sites in hemagglutinin during evolution of H3N2 human influenza A virus. *Genes Genet Syst* 86(5):287–294.
19. Munier S, et al. (2010) A genetically engineered waterfowl influenza virus with a deletion in the stalk of the neuraminidase has increased virulence for chickens. *J Virol* 84(2):940–952.
20. Air GM (2012) Influenza neuraminidase. *Influenza Other Respi Viruses* 6(4):245–256.
21. Chen W, Zhong Y, Qin Y, Sun S, Li Z (2012) The evolutionary pattern of glycosylation sites in influenza virus (H5N1) hemagglutinin and neuraminidase. *PLoS One* 7(11):e49224.
22. Rutvisuttinunt W, et al. (2015) Viral subpopulation diversity in influenza virus isolates compared to clinical specimens. *J Clin Virol* 68:16–23.
23. Matsuoka Y, et al. (2009) Neuraminidase stalk length and additional glycosylation of the hemagglutinin influence the virulence of influenza H5N1 viruses for mice. *J Virol* 83(9):4704–4708.
24. Yondola MA, et al. (2011) Budding capability of the influenza virus neuraminidase can be modulated by tetherin. *J Virol* 85(6):2480–2491.
25. Leyva-Grado VH, et al. (2014) Modulation of an ectodomain motif in the influenza A virus neuraminidase alters tetherin sensitivity and results in virus attenuation in vivo. *J Mol Biol* 426(6):1308–1321.
26. Lee YN, Lee YT, Kim MC, Gewirtz AT, Kang SM (2016) A novel vaccination strategy mediating the induction of lung-resident memory CD8 T cells confers heterosubtypic immunity against future pandemic influenza virus. *J Immunol* 196(6):2637–2645.
27. Nachbagauer R, et al. (2016) Age dependence and isotype specificity of influenza virus hemagglutinin stalk-reactive antibodies in humans. *MBio* 7(1):e01996–e15.
28. He B, et al. (2015) Adenovirus-based vaccines against avian-origin H5N1 influenza viruses. *Microbes Infect* 17(2):135–141.
29. van de Sandt CE, et al. (2015) Differential recognition of influenza A viruses by M158-66 epitope-specific CD8+ T cells is determined by extraepitopic amino acid residues. *J Virol* 90(2):1009–1022.
30. He F, Leyrer S, Kwang J (2016) Strategies towards universal pandemic influenza vaccines. *Expert Rev Vaccines* 15(2):215–225.
31. Berthoud TK, et al. (2011) Potent CD8+ T-cell immunogenicity in humans of a novel heterosubtypic influenza A vaccine, MVA-NP+M1. *Clin Infect Dis* 52(1):1–7.
32. Sridhar S, et al. (2013) Cellular immune correlates of protection against symptomatic pandemic influenza. *Nat Med* 19(10):1305–1312.
33. Pica N, Palese P (2013) Toward a universal influenza virus vaccine: Prospects and challenges. *Annu Rev Med* 64:189–202.
34. Impagliazzo A, et al. (2015) A stable trimeric influenza hemagglutinin stem as a broadly protective immunogen. *Science* 349(6254):1301–1306.
35. Hoffmann E, Neumann G, Kawaoka Y, Hobom G, Webster RG (2000) A DNA transfection system for generation of influenza A virus from eight plasmids. *Proc Natl Acad Sci USA* 97(11):6108–6113.
36. Benton DJ, Martin SR, Wharton SA, McCauley JW (2015) Biophysical measurement of the balance of influenza a hemagglutinin and neuraminidase activities. *J Biol Chem* 290(10):6516–6521.
37. Wu ZL, Ethen C, Hickey GE, Jiang W (2009) Active 1918 pandemic flu viral neuraminidase has distinct N-glycan profile and is resistant to trypsin digestion. *Biochem Biophys Res Commun* 379(3):749–753.
38. Hensley SE, et al. (2009) Hemagglutinin receptor binding avidity drives influenza A virus antigenic drift. *Science* 326(5953):734–736.
39. Budimir N, et al. (2012) Induction of heterosubtypic cross-protection against influenza by a whole inactivated virus vaccine: The role of viral membrane fusion activity. *PLoS One* 7(1):e30898.
40. Lutz MB, et al. (1999) An advanced culture method for generating large quantities of highly pure dendritic cells from mouse bone marrow. *J Immunol Methods* 223(1):77–92.